

Effect of MWCNT on the performances of the rounded shape natural graphite as anode material for lithium-ion batteries

Sang-Young Lee · Jong Hyeok Park · Pilkyu Park · Jong Hun Kim · Soonho Ahn ·
Kyeong-Jik Lee · Hyung-Dong Lee · Jae-Sung Park · Deok-Hyeong Kim ·
Yeon Uk Jeong

Received: 21 April 2009 / Revised: 14 June 2009 / Accepted: 18 June 2009 / Published online: 9 July 2009
© Springer-Verlag 2009

Abstract Multi-walled carbon nanotube (MWCNT) with bundle-type morphology was introduced as a new functional additive working as a particle connector or an expansion absorber in the anodes of lithium-ion batteries. By controlling the dispersion process, the MWCNT bundles were successfully divided and dispersed between the host particles. The composite anode consisting of rounded shape natural graphite and 2 wt.% of MWCNT exhibited the capacity of 300 mAh g⁻¹ at 3 C rate and excellent cyclability. The well-dispersed MWCNT bundles made it possible to relieve the large strains developed at high discharge C rates and to keep the electrical contact

between the host particles during repeated intercalation/deintercalation. This study has also emphasized that when high C-rate applications of lithium-ion batteries are targeted, it is important to get optimum content of MWCNT as well as uniform dispersion of their bundles in the composite anodes.

Introduction

Various types of carbon materials have been investigated for anode materials of rechargeable lithium-ion batteries for more than a decade. Depending on their structures and properties, they are classified as natural graphite, synthetic graphite, hard carbon, coke, carbon fibers, and carbon nanotubes. Among them, mesocarbon-microbead (MCMB), a representative example of the synthetic graphite, was commercialized for an anode material because its spherical shape and uniform size give the high packing density and the reversible electrochemical behaviors [1]. Recently, for the concerns of energy density and cost, natural graphite has replaced synthetic graphite. Among the approaches to improve the energy density, one is to increase gravimetric capacity (milliampere hour per gram) of the materials themselves. For example, natural graphite anodes are known to offer larger specific capacity (~360 mAh g⁻¹) than synthetic graphite due to their highly graphitized layers. Another way is to increase the packing density of the electrode by mechanically pressing the electrode. However, too excessive compression of electrodes tends to deteriorate diffusion rates and rate capabilities. Basically, the highly crystallized natural graphite has a flake or shuttle shape, and the basal planes of hexagonal layer structure in the pressed natural graphite orient in parallel with current collectors; thus, intercalation of lithium ions into graphite

S.-Y. Lee
Department of Chemical Engineering,
Kangwon National University,
Chuncheon, Gangwon-do 200-701, South Korea

J. H. Park
Department of Chemical Engineering, Sungkyunkwan University,
Suwon, Gyeonggi-do 440-746, South Korea

P. Park · J. H. Kim · S. Ahn
Batteries Research & Development, LG Chem,
Research Park,
Daejeon 305-380, South Korea

K.-J. Lee · H.-D. Lee
SODIFF Advanced Materials Co., Ltd.,
Yeongju, Gyeongsangbuk-do 750-080, South Korea

J.-S. Park
Vitzrocell Co., Ltd./R & D Center,
Yesan, Chungcheongnam-do 340-861, South Korea

D.-H. Kim · Y. U. Jeong (✉)
School of Materials Science and Engineering,
Kyungpook National University,
Daegu 702-701, South Korea
e-mail: jeong@knu.ac.kr

layers is hampered. In an attempt to improve the orientation and intercalation concerns of natural graphite in the highly pressed electrodes, new processes to make its shape rounded and random-oriented were developed. This round-

ed shape was achieved by rolling the graphene layers of natural graphite [2, 3]. Therefore, the pressing limit was liberated and the volumetric energy density could be dramatically increased. On the other hand, repeated three-

Fig. 1 SEM photographs of various anodes after roll pressing: **a** MCMB, **b** MWCNT, **c** flake-shaped natural graphite (unpressed), **d** flake-shaped natural graphite, **e** cokes, **f** cokes+0.7 wt.% of MWCNT, **g** hard carbons, **h** hard carbons+0.7 wt.% of MWCNT, **i** rounded shape natural graphite+0.7 wt.% of MWCNT, **j** rounded shape natural graphite+2 wt.% of MWCNT

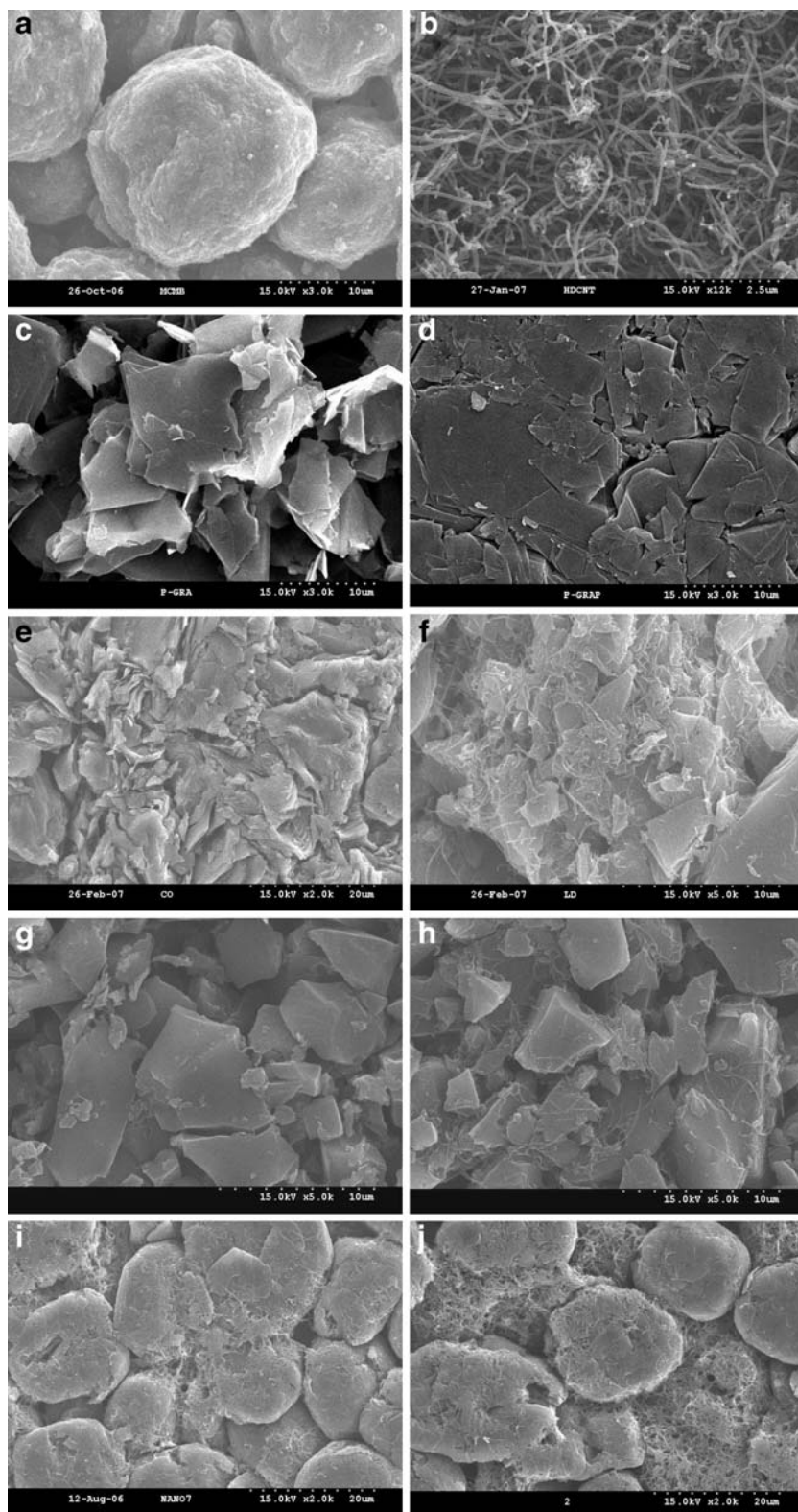


Table 1 Densities and electrochemical properties of various anodes (after roll pressing)

Materials	Electrode density (g/cm ³)	Initial efficiency (%)	Discharge capacity at 3 C/discharge capacity at 0.2 C (%)
MCMB	1.37	94.8	78.9
MWCNT	1.03	27.8	82.7
Coke	0.62	82.4	91.1
Coke+0.7 wt.% MWCNT	0.59	80.4	91.5
Hard carbon	0.96	64.8	68.1
Hard carbon+0.7 wt.% MWCNT	0.92	64.5	73.0
Flake natural graphite (unpressed)	0.54	91.1	99.5
Flake natural graphite	1.72	92.7	87.2
Rounded natural graphite	1.72	94.7	80.1
Rounded natural graphite+0.7 wt.% MWCNT	1.53	92.2	88.4
Rounded natural graphite+2.0 wt.% MWCNT	1.40	90.8	97.0
Rounded natural graphite+5.0 wt.% MWCNT	1.23	87.3	97.0

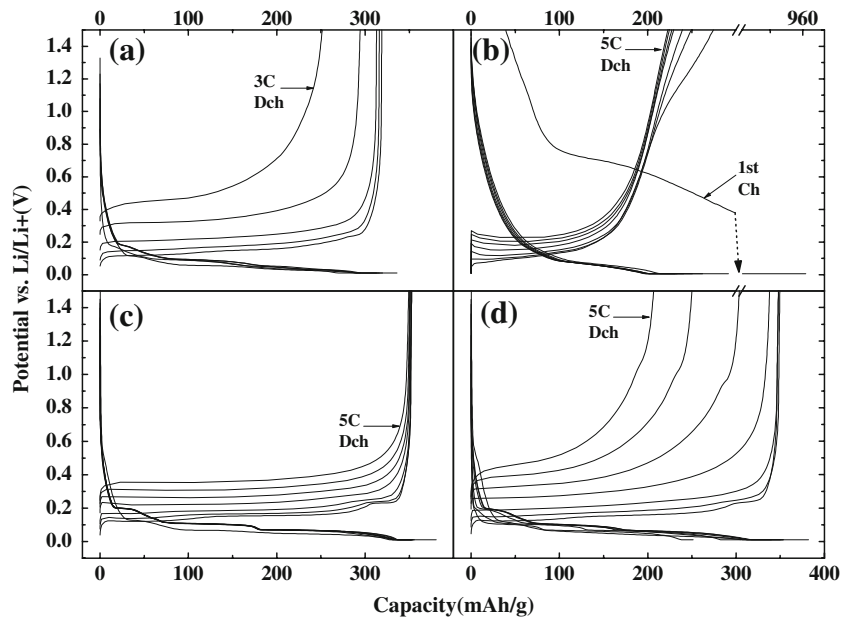
dimensional expansions and contractions of rounded particles during intercalation/deintercalation cause the contact problems between particles in the electrode. Furthermore, the longer and curved diffusion paths in the pressed electrodes might bring negative effects on ionic and electronic conductivities. Therefore, to overcome these drawbacks of electrodes, development of new functional additives for a particle connector or an expansion absorber in the electrodes is greatly needed.

Since the discovery of carbon nanotubes (CNTs), their applications to energy storage devices have been highly issued. CNTs as an anode material of lithium-ion batteries give large irreversibility for the first cycle due to their high specific surface area [4]. On the other hand, for electrical double layer capacitor application, CNTs have lower capacitance than conventional activated carbons [5]. The

dispersion of CNT in the matrix materials has been considered as a key challenge to maximize the unique properties of CNT [6–10]. Many works on the electrochemical properties of composite electrodes consisting of CNT and metal oxides were reported. For example, the composites of single-walled carbon nanotube and vanadium oxides improved the specific capacities at high discharge rates [11], and the multi-walled carbon nanotube (MWCNT) as a particle connector in the LiCoO₂ electrode was effective for capacity retention [12].

Natural graphite with rounded shape has been of interest for application to portable electronic devices requiring high energy densities; however, this has been accompanied by concerns for its C-rate capabilities. The present work demonstrates the effects of MWCNT as a functional additive on electronic, ionic, and electrochemical properties

Fig. 2 Charge and discharge profiles at various discharge rates of 0.2, 0.5, 1.0, 2.0, 3.0, 4.0, and 5.0 C for **a** MCMB (pressed), **b** MWCNT (pressed), **c** flake-shaped natural graphite (unpressed), and **d** flake-shaped natural graphite (pressed)



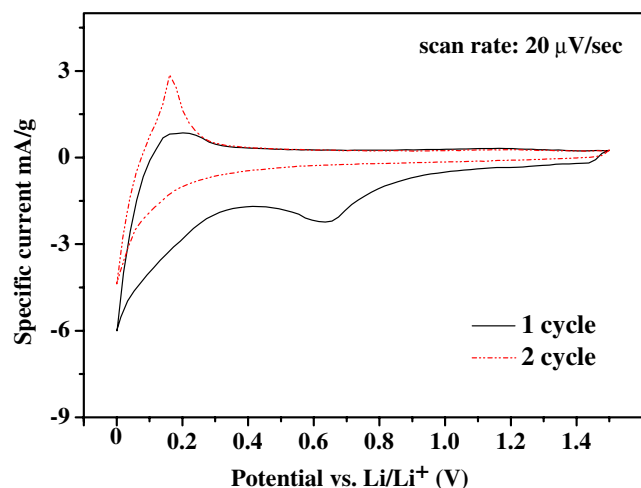


Fig. 3 Cyclic voltammogram for MWCNT

of carbon-based anodes. More importantly, their influences on the high C-rate performances of the rounded natural graphite are one of our key interests.

Experimental

The vapor growth method was used to prepare MWCNT obtained from Nanokarbon in Korea. The length and outer and inner diameters were 10–20 μm and 60–80 and 30–50 nm, respectively. Including the rounded natural graphite with diameter of 18–20 μm , various types of carbon materials were provided by Sodiff Advanced Materials, Co., Korea. Binder solutions were prepared by mixing polyvinylidene fluoride (PVDF) in *N*-methyl-2-pyrrolidone (NMP). MWCNT samples were dispersed in NMP by a homogenizer, followed by the addition of binder solutions, and mixed at 5,000 rpm for 10 min. The determined amounts of carbon materials were added in the prepared MWCNT/binder solution and mixed by a homogenizer at 5,000 rpm for another 10 min. Additional NMP was added to adjust optimum viscosity, and the weight ratio of carbon materials to PVDF binder was set at 90:10. The composite slurries were coated onto copper current collectors with a thickness of 18 μm , followed by drying in an oven for 30 min at 120°C. The electrode thickness after roll pressing was measured around 80–90 μm .

For electrochemical measurements, coin cells were assembled in an argon-filled glove box. A lithium metal foil was used as the counter electrode and a polypropylene film with the thickness of 18 μm was used as a separator. A 1-M LiPF₆ in a mixture of ethylene carbonate, ethyl methyl carbonate, and diethyl carbonate was used as a liquid electrolyte. For charge/discharge tests, a Toyo battery tester was used. The cycle range was 0.01–1.5 V vs. Li/Li⁺ and 1 C rate was 300 mAh g⁻¹. The charge tests were carried

out by constant current (0.2 C to 0.01 V), followed by constant voltage (0.01 C cut-off). To examine the discharge rate capabilities, constant current in the range of 0.2–5.0 C was applied to a cell one after another. Occasionally, a shallow short due to dendrite growth from lithium metal happened at a current density of 8–9 mA cm⁻², and we excluded these data to avoid misunderstanding. Meanwhile, by using a polyester film as a coating substrate for the composite slurry, the electrical conductivities of electrodes were measured and analyzed by the van der Pauw method.

Results and discussion

Figure 1 shows the morphologies for various anodes after pressing. To improve electrochemical performances in lithium-ion batteries, electrical conduction as well as ionic diffusion should be enhanced. It is known that electrical properties depend on the bonding characteristics related with the degree of graphitization of carbon. Natural graphite has better electronic conduction than synthetic graphite as more sp² hybrid orbitals allow π bonds on highly graphitized layers. On the other hand, disordered forms enable faster lithium intercalation as they offer shorter ionic diffusion paths. The densities and electrochemical properties of various anodes were summarized in Table 1.

The charge and discharge characteristics of MCMB, MWCNT, and flake-shaped natural graphite are shown in Fig. 2. In the case of MWCNT anodes, 50 wt.% of binder was used compared to 10 wt.% for the other anodes. The MWCNT anodes show a large difference in the first charge and discharge capacities, which might be due to the surface reaction on the MWCNT with high surface area. The cyclic voltammogram for the MWCNT anodes (Fig. 3) indicates the irreversible reaction on the surface at 0.635 V vs. Li/Li⁺.

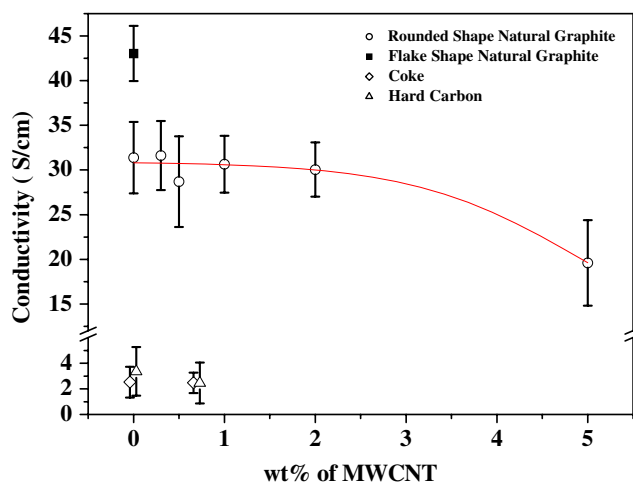
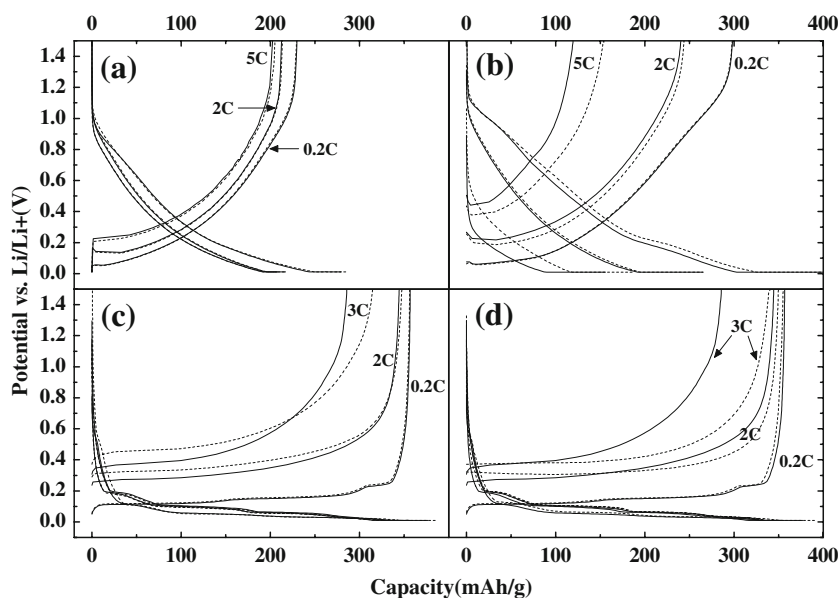


Fig. 4 Electrical conductivities of various anodes after roll pressing

Fig. 5 Charge and discharge profiles at various C rates for pressed anodes: **a** cokes (solid line) and cokes+0.7 wt.% MWCNT (dotted line), **b** hard carbons (solid line) and hard carbons+0.7 wt.% MWCNT (dotted line), **c** rounded shape natural graphite (solid line) and rounded shape natural graphite+0.7 wt.% MWCNT (dotted line), and **d** rounded shape natural graphite+2 wt.% MWCNT (dotted line) and rounded shape natural graphite+0.7 wt.% MWCNT (dotted line)



From Table 1 and Fig. 2c, it was observed that the unpressed anode of flake-shaped natural graphite has an electrode density of 0.54 g cm^{-3} and shows excellent rate capability. On the other hand, from Table 1 and Fig. 4, it is found that the pressed anode of flake-shaped natural graphite has 1.72 g cm^{-3} of electrode density and high electrical conductivity. The pressed flake graphite and MCMB exhibit low rate capabilities due to the low ionic diffusion rate, which are shown in Fig. 2a, d. Figures 2 and 5 show rounded shape graphite, and though the pressed anode shows high density, it exhibits the higher C-rate capability than the pressed flake graphite and MCMB. This is due to the random orientation of rolled graphene layers in the rounded shape natural graphite.

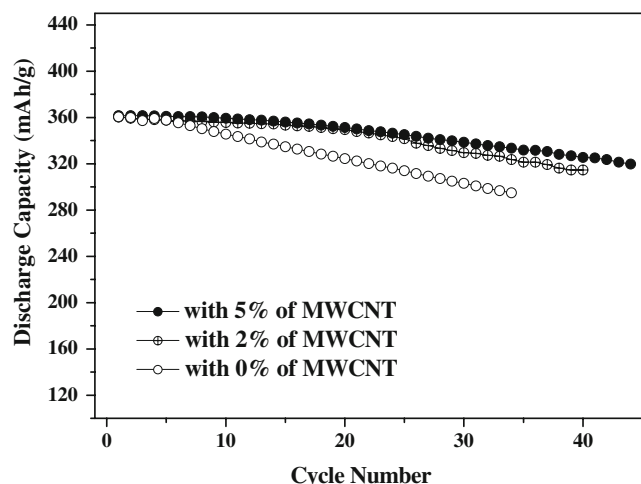


Fig. 6 Cycle performances of the anodes for rounded shape natural graphite with various contents of MWCNT

Generally, MWCNTs have bundle-type morphologies, and it is not easy to individually separate the bundles. In order to improve their degree of separation, sonication is

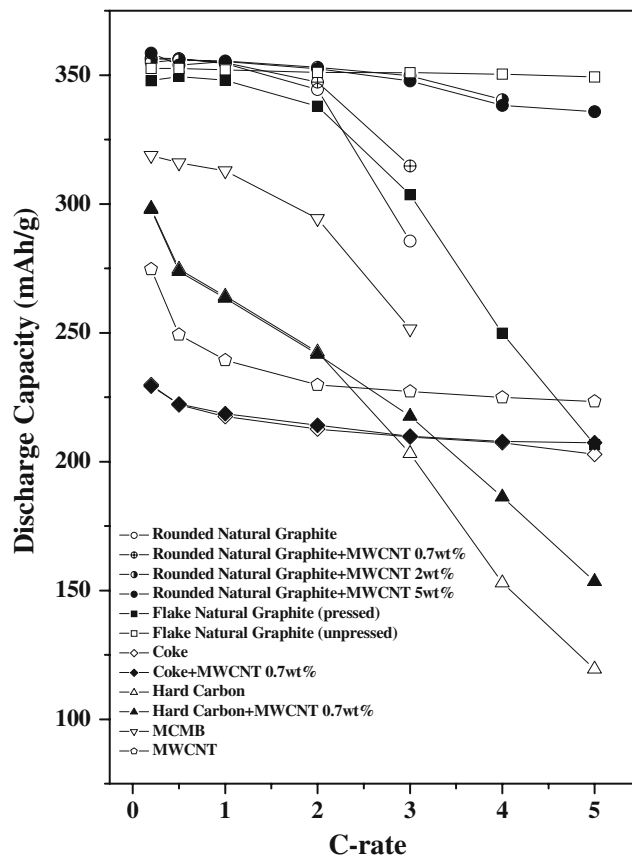


Fig. 7 Gravimetric discharge capacities of different C rates for various anodes after roll pressing

often employed. However, poor control of sonication treatment, for example, excessively high power and long time, results in the generation of defects and the complete fragmentation of carbon nanotubes. Our strategy is to divide the agglomeration of bundles and to disperse the separated bundles between the anode materials. Even though an individual carbon nanotube has excellent electrical conductivity, the bundle itself has a large contact resistance. Figure 4 exhibits that the electrical conductivities of rounded shape graphite are lower than those of flake-shaped graphite and higher than those of hard carbon and coke. It is observed that the conductivities of rounded shape natural graphite decrease with the increase of MWCNT content. In spite of the low electrical conductivities of rounded natural graphite-based composite anodes, their high C-rate capacities exceed those of anodes without MWCNT, as shown in Fig. 5c, d. The rounded shape of natural graphite has been due to the rolled graphene layers, yielding the relatively long ionic diffusion paths. In the pressed anodes, extraction of lithium ions from the graphene layers at high C rates is inevitably accompanied by the buildup of large strains. This volume change is likely to be absorbed by the buffer action of MWCNT between the graphite particles. This phenomenon becomes remarkable at the higher C rates, and it is found that the composite anodes with 2 wt.% of MWCNT and 5 wt.% of MWCNT show similar C-rate capabilities. Figure 5a, b exhibits that a similar behavior was also obtained in the hard carbon-based composite anodes, but not observed in the coke-based composite anodes. This might be due to the low electrode density of cokes. Table 1 reveals that the Coulomb efficiency of first discharge capacity to charge capacity and the densities of anodes decreased with the increase of the MWCNT content.

Figure 6 compares the cyclability for the various anodes, where the 0.2 C of constant current (CC)–constant voltage and the 1.0 C of CC were used for the charge and discharge rates, respectively. The cyclability is considered to reflect the degree of deterioration of constituents during cell operation. The buffer action of the well-distributed MWCNT in the composite anodes facilitates the migration of lithium ions and the electrical contact between the anode materials. Figure 7 summarizes the gravimetric discharge capacities of various C rates for various anodes.

Conclusion

The effect of MWCNT as a new functional additive on the C-rate capabilities of composite anodes has been investigated. The MWCNT additives were observed to act as a particle connector or an expansion absorber in the anodes of lithium-ion batteries. By controlling the dispersion process, the MWCNT bundles were successfully divided and dispersed between host particles. The rounded graphite with 2 wt.% of MWCNT exhibited high C-rate capacity (300 mAh g⁻¹ at 3.0 C rate) even at high electrode density. The well-dispersed MWCNT bundles enabled to relieve the large strains developed at high discharge C rates and to keep the electrical contact between the host particles during repeated intercalation/deintercalation. For enhanced high rate capabilities of lithium-ion batteries, it is important to apply the optimum content of MWCNT as well as careful dispersion of their bundles in the composite anodes.

Acknowledgments This research was supported by LG Chem in Korea. The authors greatly appreciate the financial support and insightful discussions.

References

1. Mabuchi A, Tokumitsu K, Fujimoto H, Kasuh T (1995) *J Electrochem Soc* 142:1041
2. Yoshio M, Eang H, Fukuda K (2003) *Angew Chem Int Ed* 42:4203
3. Ohzeki K, Saito Y, Golman B, Shinohara K (2005) *Carbon* 43:1673
4. Claye AS, Fischer JE, Huffman CB, Rinzler AG, Smalley RE (2000) *J Electrochem Soc* 147:2845
5. Niu C, Sichel EK, Hoch R, Moy D, Tennent H (1997) *Appl Phys Lett* 70:1480
6. Wang H, Hobbie EK (2003) *Langmuir* 19:3091
7. Maeda Y, Kimura SI, Hirashima Y, Kanda M, Lian Y, Wakahara T, Akasaka T, Hasegawa T, Tokumoto H, Shimizu T, Kataura H, Miyauchi Y, Maruyama S, Kobayashi K, Nagase S (2004) *J Phys Chem B* 108:18395
8. Islam MF, Rojas E, Bergey DM, Johnson AT, Yodh AG (2003) *Nano Lett* 3:269
9. Vaisman L, Marom G, Wagner HD (2006) *Adv Funct Mater* 16:357
10. Stephenson JJ, Hudson JL, Azad S, Tour JM (2006) *Chem Mater* 18:374
11. Sakamoto JS, Dunn B (2002) *J Electrochem Soc* 149:A26
12. Sheem K, Lee YH, Lim HS (2006) *J Power Sources* 158:1425